Available on CMS information server

CMS NOTE -2009/019

The Compact Muon Solenoid Experiment

CMS Note

Mailing address: CMS CERN, CH-1211 GENEVA 23, Switzerland

16 July 2009 (v4, 11 January 2010)

MARS15 Simulation Studies in the CMS Detector of Some LHC Beam Accident Scenarios

P.C. Bhat, N.V. Mokhov, S.I. Striganov

Fermi National Accelerator Laboratory, IL 60510, U.S.A.

A.P. Singh

Panjab University, Chandigarh, India

Abstract

The CMS tracker, made of silicon strips and pixels and silicon-based electronics, is vulnerable to effects of radiation exposure during the LHC operation. Of much concern is the potential for damage from a high instantaneous dose to the pixel detectors and electronics located only a few centimeters from the beam in the event of a fast accidental beam loss. One of the worst case scenarios for such a beam loss is an unintended firing of an abort kicker module, referred to as the kicker pre-fire. MARS15 simulation studies of radiation loads in CMS for the kicker pre-fire scenario are described in this paper. It is found that, in a kicker pre-fire accident, in a time span of about 100 ns, the innermost pixel layer may see a radiation dose of about 0.02 Gy - equivalent to a fluence of $\sim 6 \times 10^7$ MIPs/cm^2. No discernible damage to the pixel detectors or the electronics were seen at these levels of fluence in recent beam tests. We note that the dose is about 1000 times smaller than previously estimated before tertiary collimators were introduced in sector 5-6. We also present here a brief discussion of other accident scenarios. Our studies show that a mis-steered 450 GeV beam hitting a TAS absorber in CMS at $\sim$19 m from the interaction point can produce 0.5 Gy per pilot bunch of 10^{11} protons. We strongly urge that procedures be put in place to eliminate the risk of this accident.

1. Introduction

The CMS all-silicon tracker [1] has been designed to operate efficiently for at least ten years in the high-radiation environment of the LHC proton-proton collisions at the design luminosity. The inner pixel layer, however, will need a replacement or be augmented after operation of a few years at the design luminosity. The outer detectors of the CMS – the calorimeters and the muon system, should last and perform well beyond the ten years. The tracker is also expected to withstand the accompanying machine-induced background (MIB), originating from interactions of beam halo protons on limiting apertures in the machine and interactions of circulating protons with remnant gas molecules in the beam pipe [2]. Fast accidental beam losses, however, pose serious risks to the safety of the tracker. Even though the expected integrated radiation from accidental beam losses are small, very large instantaneous ionization due to fast losses can cause breakdown in detector components resulting in irreversible damage. The inner layers of the pixel detector located only a few centimeters away from the beam orbit, are, by far, the most vulnerable.

A schematic layout of the LHC machine is shown in Fig. 1. It highlights the locations of the interaction points, the four experiments – CMS, ALICE, ATLAS, and LHCb, and beam collimators in the extensive collimation system, especially in the betatron (IP7) and momentum cleaning (IP3) insertions. During nominal operation at 7 TeV, each of the beams has total energy of about 340 MJ, which, in an accident, can cause severe damage to the machine and detector components. The possible beam accident scenarios in the LHC include an unsynchronized beam abort, an abort kicker module pre-fire (which triggers an unsynchronized beam abort) and mis-injected proton bunches. A single abort module kicker pre-fire, which is likely to happen with some frequency (the guess is ~1 per year), is thought to be the worst case accident scenario that can affect pixel safety [3]. Detailed Monte-Carlo simulations and analysis of this scenario are performed. The interactions of beam protons and secondaries with the accelerator and detector elements are modeled using the MARS15 Monte-Carlo code [4]. As described in Ref. [2], the proton losses on the IP1 and IP5 tertiary collimators were calculated by T. Weiler using a collimation version of SixTrack [5]. Detailed results of the simulations in terms of absorbed radiation dose as well as fluences and energy spectra of various particles are presented in this paper. In particular, the impact of such an accident on the inner layers of the pixel detector are considered and discussed.

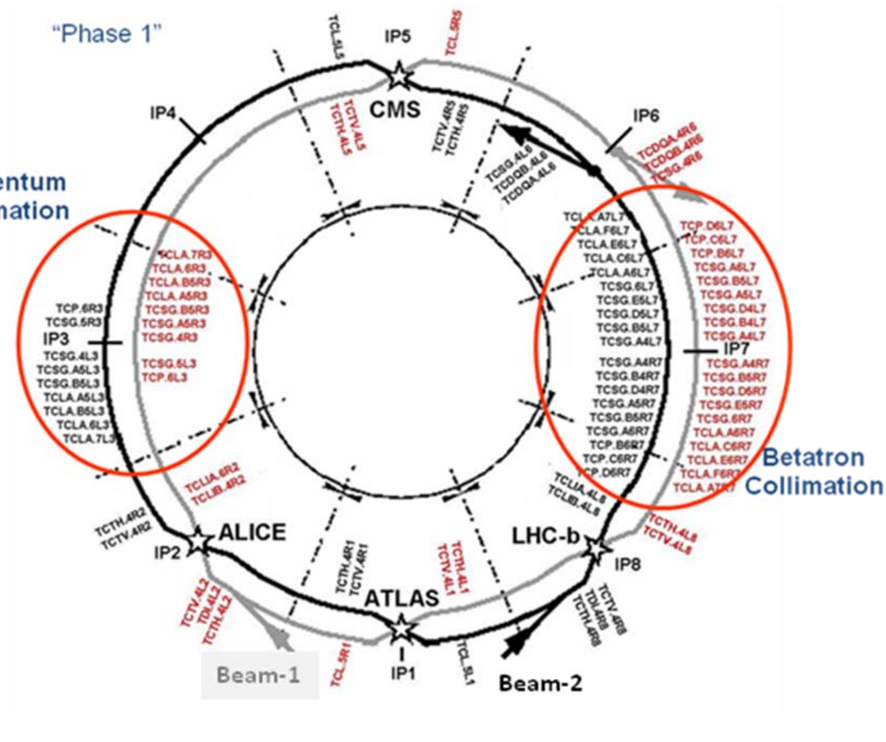

Fig. 1. A schematic layout of the LHC showing the interaction points, locations of the four experiments and the collimators around the LHC ring. The beam abort system is located at IP6

2. Kicker Pre-fire at 7 TeV

Since machine protection from the very high-intensity beams is of paramount importance, LHC has an extensive and sophisticated multi-stage beam collimation system. Locations of the important collimators around the ring are shown in Fig. 1. Two proton beams, denoted Beam-1 and Beam-2, circulate in opposite directions in the machine and collide at the designated interaction points of the LHC experiments. The CMS detector is housed at the Interaction Point 5 (IP5). The LHC beam abort system consists of 14 pulsed magnets with a rise time of 3 μs. The abort system is located in IP6, in the proximity of CMS at IP5. During a normal intended beam abort, the abort system is triggered during the 3 μs abort gap in the circulating beam. This results in a clean extraction of the beam - with no impact on the experiments - to an external graphite dump. However, there is a finite probability that one of the abort kicker modules can fire accidentally at an unintended time. If this happens, then the remaining 13 modules are triggered by the machine protection system to fire within 700 ns to dump the beam [2]. This accidental scenario is referred to as a single module kicker pre-fire. Since the abort kicker modules need some time (~3 μs) to reach their normal strength, some number of bunches from Beam-2 will be mis-steered as they are approaching CMS and can hit the machine elements downstream of IP6. As was first shown in [3], the impact on the machine and collider detectors – without a multi-component protection system in IP6 [6] - can be disastrous. These bunches can be lost in the IP1 and IP5 tertiary collimators and low-beta regions, causing considerable radiation loads to CMS and ATLAS. At the end of the first turn, the beam will get completely extracted to the beam dump. For Beam-1, the same abort kickers and dump in IP6 are used but the impact on CMS of mis-steered Beam-1 bunches is far less compared to Beam-2, since they are travelling away from CMS and so will be absorbed mostly in the machine collimation system before they come around the ring to IP5.

The impact on CMS of the deflected bunches from Beam-2 on the first turn when a kicker module pre-fires is studied here. As described in Ref. [2], the scenario considers a kicker pre-fire at 7 TeV beam energy, assuming a $\pi/2$ phase advance between the pre-firing kicker magnet and the tertiary horizontal collimator (TCTH), located at ~148 m from IP5, downstream of the kickers but upstream of the low-beta quadrupole triplets in IP5. This relative phase results in the maximum deflection of the beam at the entrance of the tertiary collimator [7], and hence represents the worst case scenario for this accident. Furthermore, as in [2], it is assumed that the dump protection collimators in IP6 are not optimally aligned so that protons with a betatron amplitude between 8.3σ (nominal setting of the collimator at 7 TeV and $\beta^* = 0.55$ m in IP5) and 10.28 σ (aperture due to the arc) will hit the tertiary collimator (TCT) at 148 m from IP5. With proper dump protection settings, (shower absorbers TCSG at 7.5 σ and TCDQ at 8.3σ), the TCTs would, in fact, be shadowed. The main purpose of the TCTs, from the point of view of machine protection, is, indeed, to protect the low-beta quad triplets against radiation damage in case of a compromised dump protection and an irregular abort. Assuming a Gaussian beam profile for each bunch, a kick corresponding to the current in the ramping kicker magnet is used to calculate the deflection of each bunch and used as starting point for showering simulations in the accelerator elements at and downstream of the TCTH. Nominal bunch intensities of $1.15 * 10^{11}$ protons and bunch intervals of 25 ns are assumed. The kick seen by particles in each bunch is plotted as a function of time as the kicker magnet ramps, in Fig. 2, taken from Ref. [2]. Particles with a deflection below 5.08σ (μrad) pass through IP5 and may hit the IP7 collimators or are extracted after one turn, while those above 10.28σ (μrad) are assumed to be absorbed in IP6.

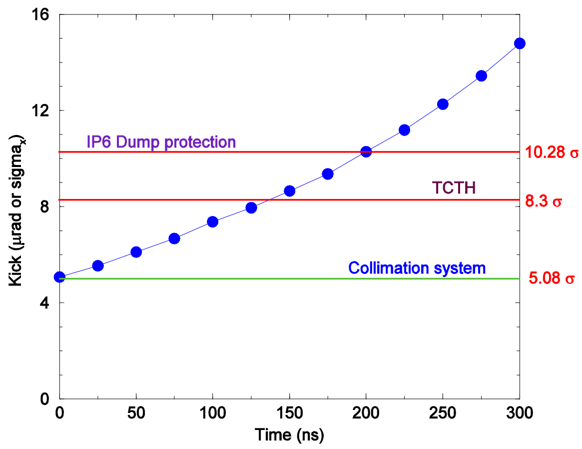

Fig. 2. Angular kick of 13 bunches at prefire of the MKD.OR6.B2 beam dump kicker module (from Ref. [2]).

3. MARS Monte-Carlo Simulations

The MARS15 [4] code is used here to simulate interactions of a mis-steered beam with the beamline elements downstream of the abort kicker as well as subsequent showering and passage of particles in the interaction region and in the CMS detector. MARS15 employs extensive Monte Carlo techniques to simulate multi-particle interactions, three-dimensional development of hadronic and electromagnetic cascades, and modelling of heavy ion, muon and low-energy neutron and photon transport in accelerator and detector components. Particles ranging in energies from a fraction of an electron volt to about 100 TeV are handled. MARS15 also supports extensive geometry and material description as well as electric and magnetic field maps, and produces results on particle fluence, energy spectra, energy deposition etc. The cutoff energies for various particles below which they are not processed further, are as follows: 100 keV for most particles, and down to thermal energies for neutrons. In this study, for reasons of efficiency, they were defined higher depending on the region under consideration. The simulations are performed in two parts – (1) the particles in the deflected bunches are used as the source particles for simulations in the accelerator region of the IR, upstream of the CMS hall, producing four-vectors of particles at the entrance of CMS hall, at Z=22.6 m; (2) simulations of interactions and passage of particles throughout the CMS detector are performed using the results from the previous step as the source. All particles with energies above 20 MeV are used in the second step. The MARS geometry of the 150-m region of IP5 – with all the machine optics, collimators, absorbers and tunnel - is shown in Fig. 3, while Fig. 4 shows the CMS detector model (only a quarter shown). The solenoidal magnetic field in the CMS detector of 4 T is implemented in a hard-edge approximation.

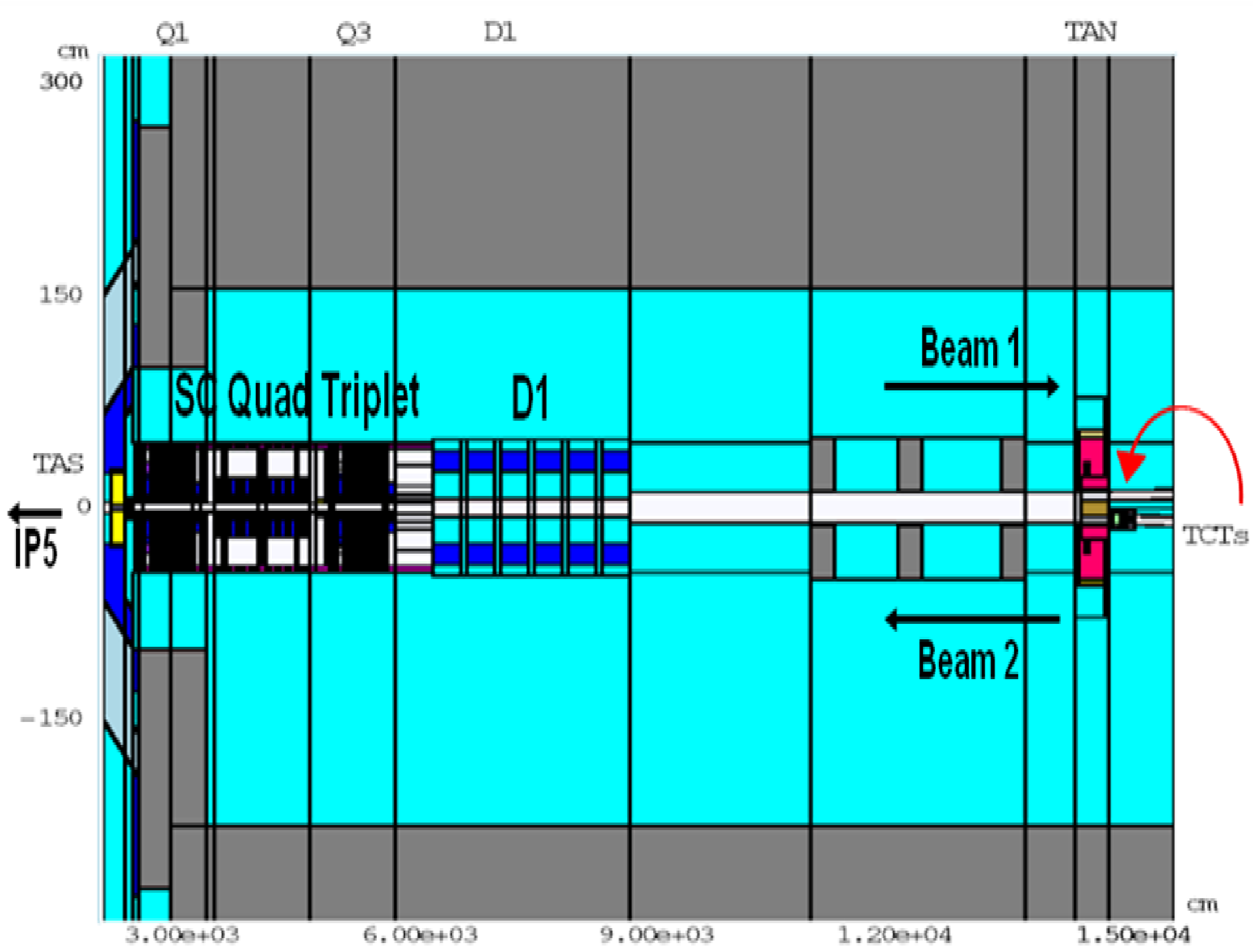

Fig. 3. The machine elements in the Interaction Region (IR5) implemented in the MARS model.

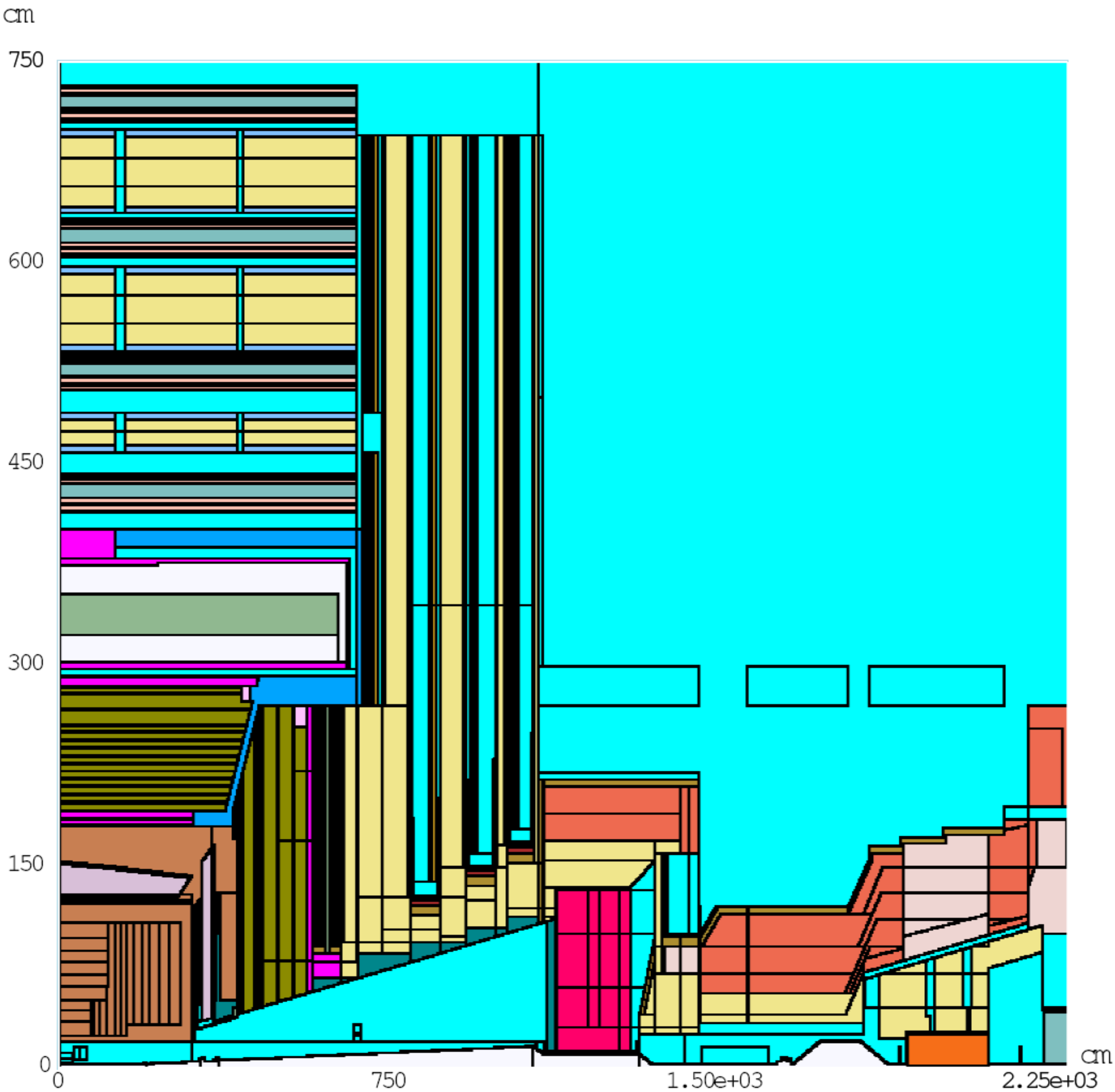

Fig. 4. The CMS detector in MARS.

4. Simulation Results in the Region Upstream of CMS

Of the thirteen deflected bunches considered (with 25 ns bunch interval), nine bunches would not be completely intercepted by the collimation or the IP6 protection system if set, sub-optimally, at 10.28σ of the beam, as discussed earlier (see Fig. 2). Some fraction of protons from these bunches will hit the TCTs and/or other elements downstream producing particle showers which continue to develop from further interactions as particles travel toward CMS. The results of MARS15 simulations in this region upstream of CMS are presented in this section in terms of the fluences and energies of various types of particles at the entrance of the CMS experimental hall, at an interface plane at z=22.6 m and transverse to the nominal beam direction. More results can be found in Ref. [2].

Fig. 5 shows the number of various types of particles (with energy> 1 GeV and within a radius of 1 m) resulting from each of the nine bunches, at the interface plane. It can be seen that most of the particle fluence into CMS comes from bunches 4 through 9. Radial distributions of the proton fluence are shown in Fig. 6. The particle fluence distributions at the interface plane are shown in Fig. 7, for various types of particles. It is seen that protons are mostly confined close to the beam direction while muons extend to very large transverse distances from the beamline. The energy-weighted particle distributions in the transverse plane for muons and protons are shown in Fig. 8. Again, one can see the energetic protons tightly clustered around the beam direction and muons spreading to larger radial distances. Fig. 9 shows energy spectra of particles approaching the CMS detector in the first meter radially outside the TAS (Target Absorber Secondaries) aperture of 1.7 cm. It is interesting to note the presence of rather energetic tails for hadrons and muons (more energetic than for tertiary halo) because of large grazing-angle events on the TCTs [2].

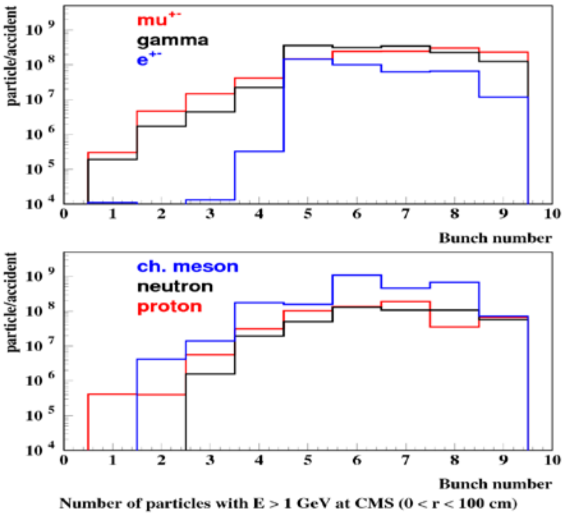

Fig. 5. Number of particles of various type at the entrance of CMS hall (Z=22.6m) originating from each of the nine un-intercepted bunches (from Ref. [2]).

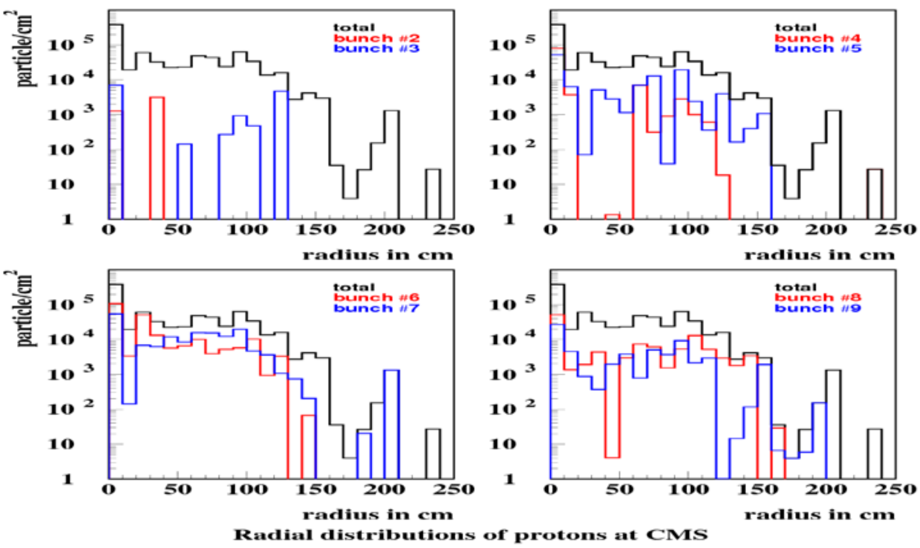

Fig. 6. Radial distributions of proton fluence at the entrance of CMS hall (at z=22.6 m, E > 1GeV). Total fluence (black histograms) is compared with contributions from specific bunches as labelled.

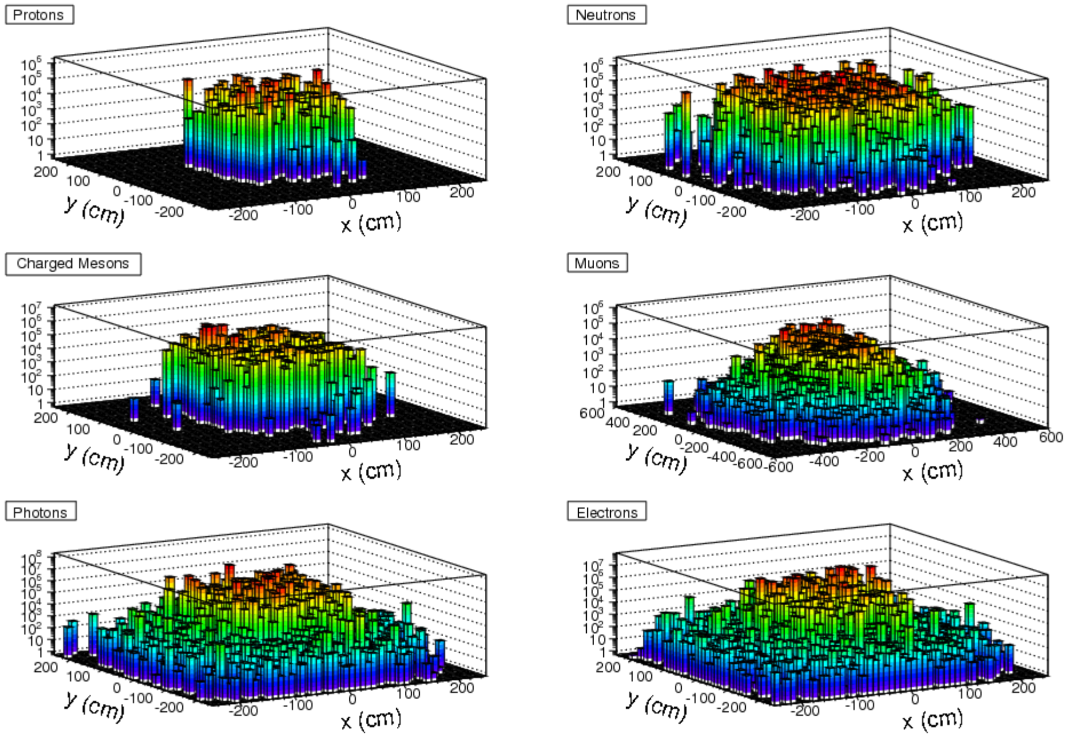

Fig. 7. Particle fluences (Particles/cm^2) at the entrance of the CMS hall. Note the symmetric, Gaussian like profile for muons (E>1 GeV) which also extends to much larger radii than for other particles.

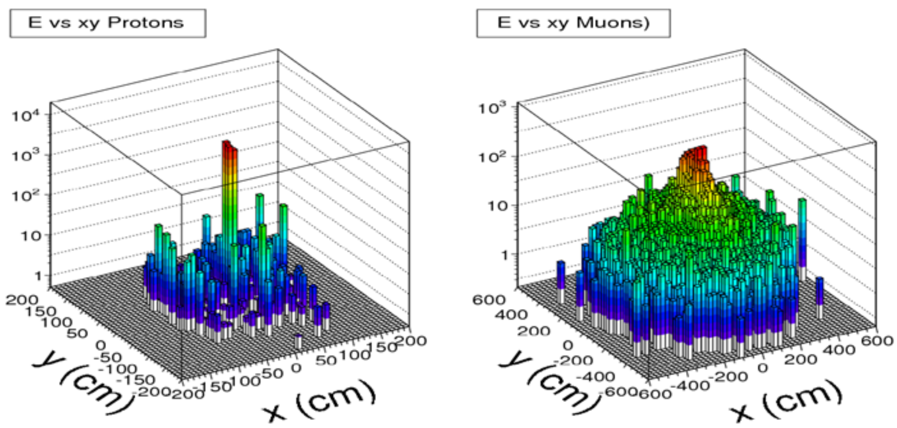

Fig. 8. Energy-weighted proton (left) and muon (right) fluences, in the transverse plane at the entrance to CMS.

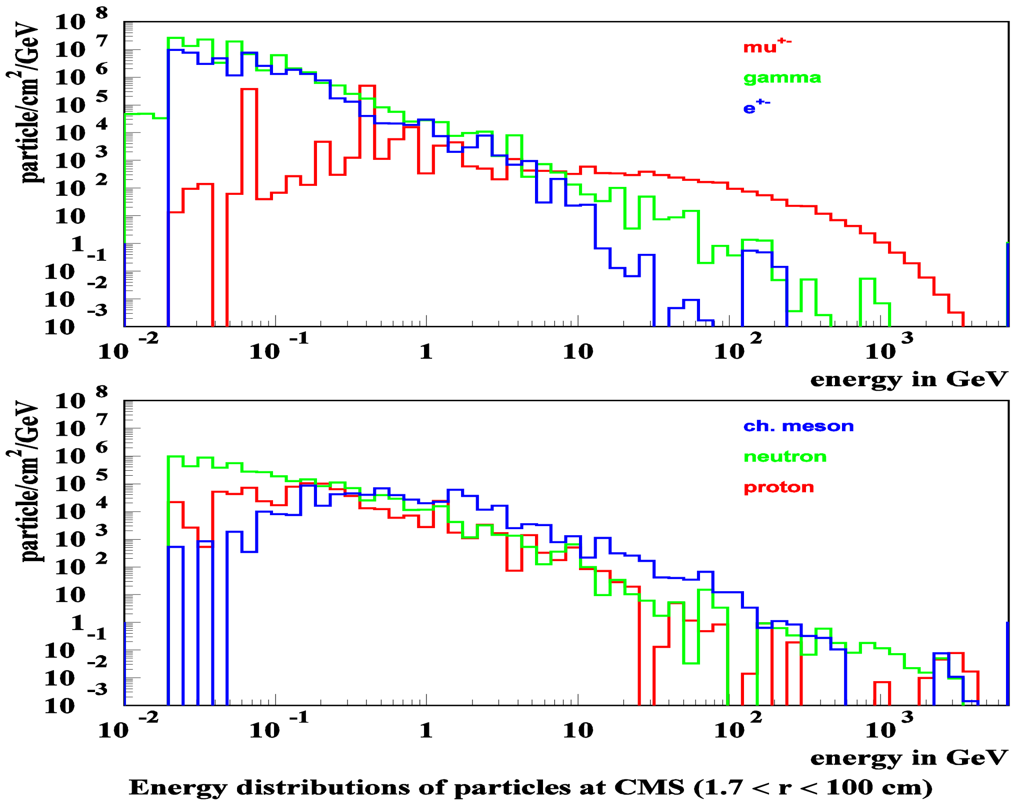

Fig. 9. Particle energy spectra at z=22.6 m from IP5 in the 1.7 < r < 100 cm region (from Ref. [2]).

5. Simulation Results in CMS

In this section, we present and discuss results of MARS simulations in the CMS detector carried out using the four-vectors of particles at z=22.6 m from IP5, discussed above, as the source. Even though our primary concern was the impact of the kicker pre-fire on the pixel detector the simulations are performed in the entire detector using the geometry shown in Fig 4. The YZ projection of the quarter of the detector is shown in the figure but cylindrical symmetry around the beam axis and mirror symmetry about the interaction point are assumed and used in simulations. Although results are presented for the entire detector, the discussion here is focused on the results for the pixel detector.

Figs. 10-12 display the azimuthally averaged 2D maps of the particle fluences calculated in the detector in the RZ-plane, for a kicker pre-fire accident, while Fig. 13 shows that for the absorbed dose. In all these plots, the beam direction is from right to left (from +z to –z). The tertiary collimators are at z=+148 m. The bins of the 2D histograms are about 20 cm along z and 6 cm in radius. The granularity of the histograms is sufficient to understand the distributions of dose and fluences throughout the detector. From Fig. 13, one sees that the most intense radiation doses are received by detector components at the upstream entrance and those that lie close to the nominal beam direction. The maximum dose in the detector components is less than 0.1 Gy per accident even in the hottest spots. In general, both dose and muon fluence have patterns spreading conically outward as the particles traverse across the detector. The muon fluence can be seen to be highest from very close to the beam pipe to about r=2.5 m and one sees the attenuation of the fluence as muons traverse through the material in the calorimeter. Charged hadrons and neutrons have patterns consistent with the material distribution in the detector.

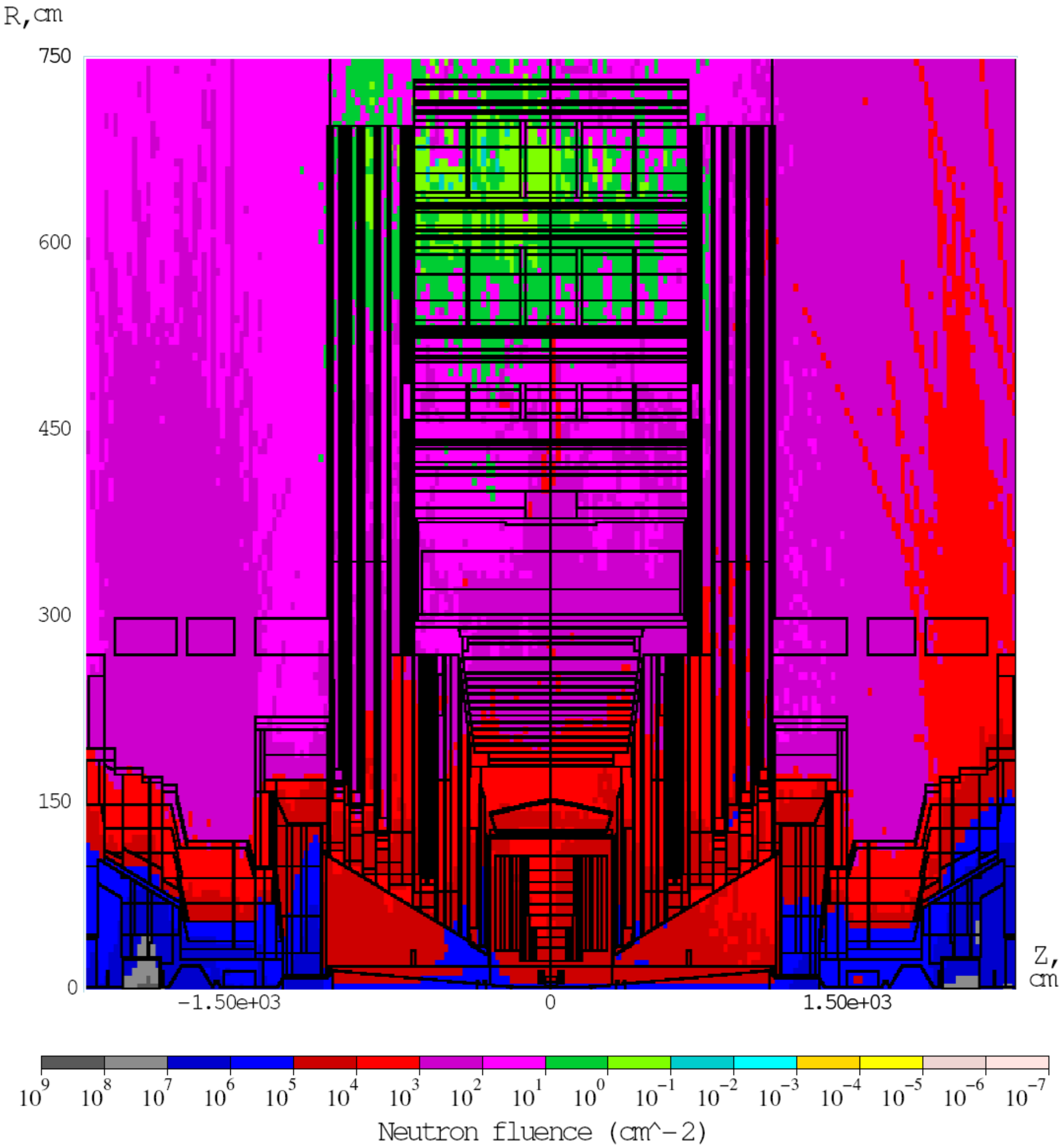

Fig. 10. Azimuthally-averaged neutron fluence isocontours (cm^{-2}) in the CMS detector for a kicker prefire accident for a 7-TeV beam going from right to left.

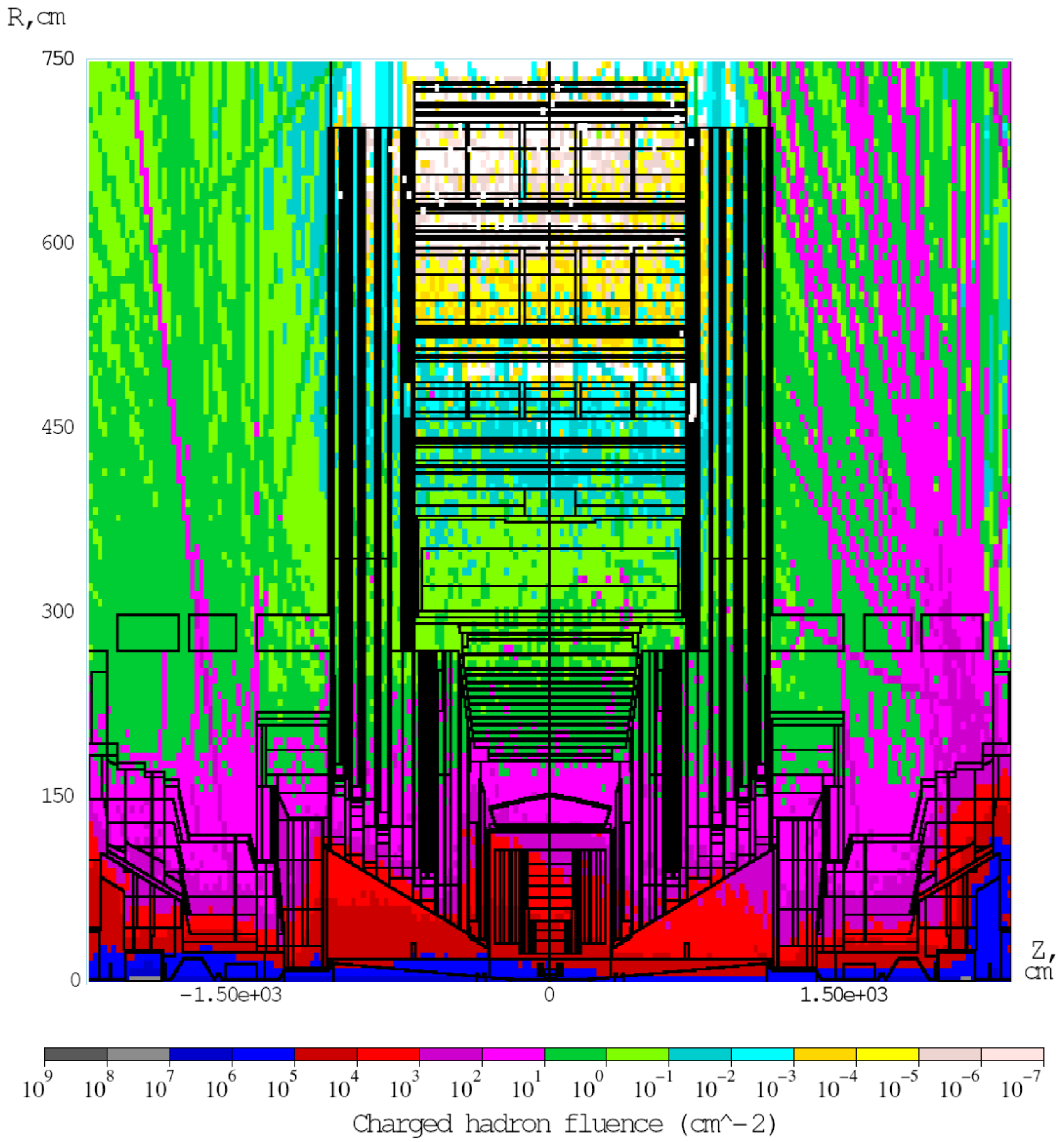

Fig. 11. Azimuthally-averaged charged hadron fluence isocontours (cm^{-2}) in the CMS detector for a kicker prefire accident for a 7-TeV beam going from right to left.

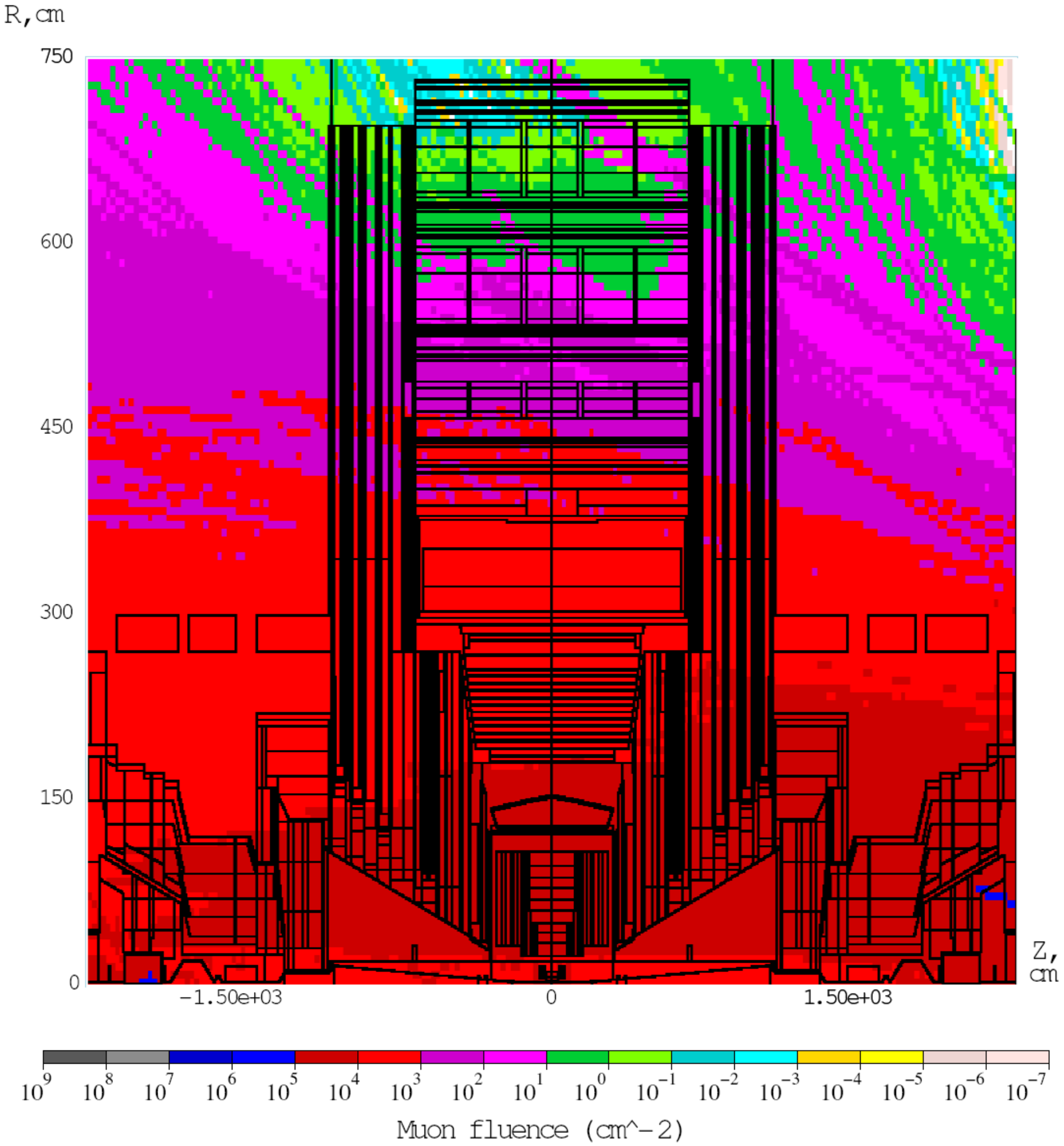

Fig. 12. Azimuthally-averaged muon fluence isocontours (cm^{-2}) in the CMS detector for a kicker prefire accident for a 7-TeV beam going from right to left.

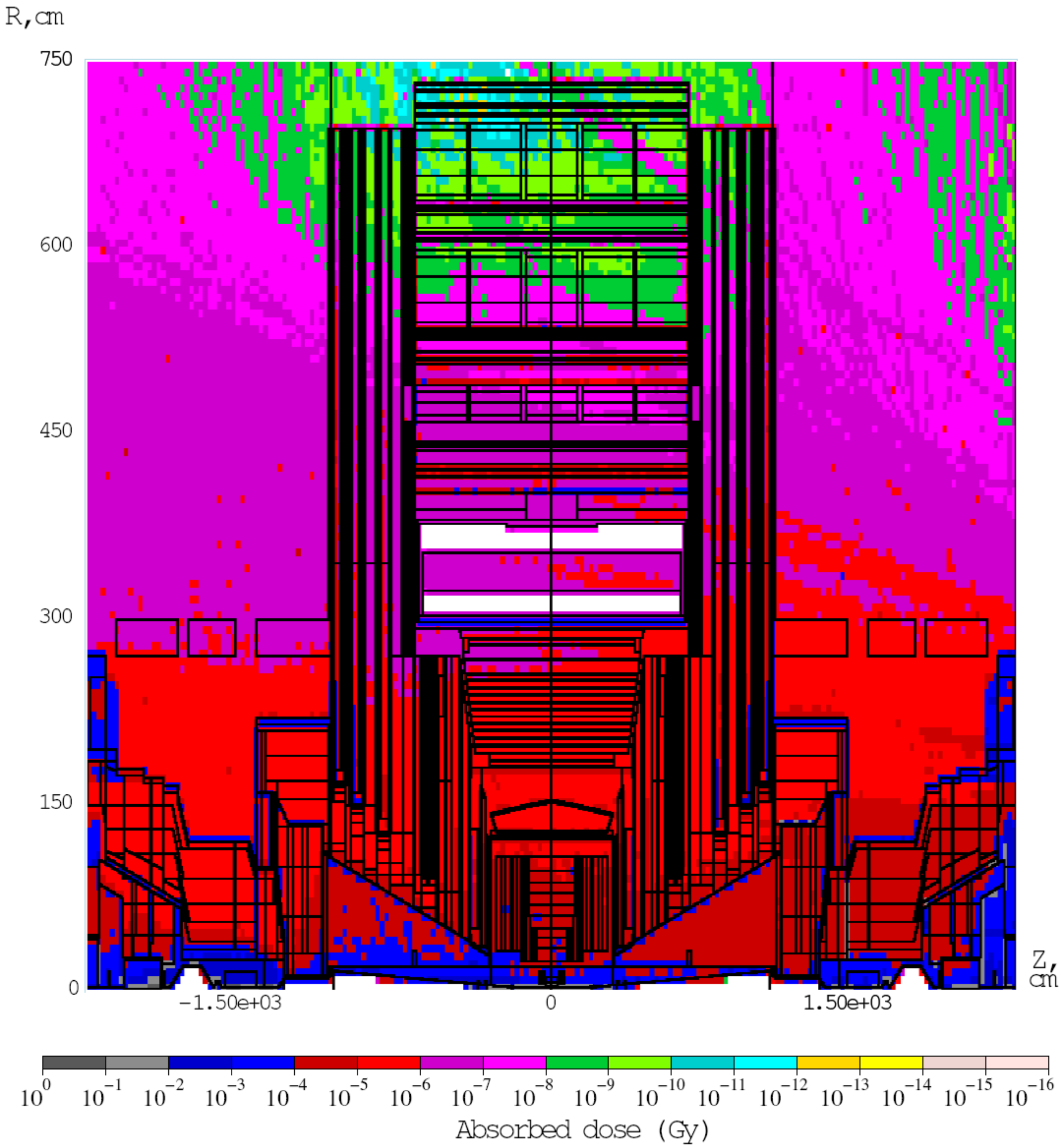

Fig. 13. Azimuthally-averaged absorbed dose isocontours (Gy) in the CMS detector for a kicker prefire accident for a 7-TeV beam going from right to left.

For more precise information, particles are scored within specified detector volumes and dose and fluences calculated. Those results are used for a closer look at the effect on the individual detectors. These doses and fluences in some representative layers of the detector are shown in Tables 1. The radial dependence of doses and fluences in the tracker are plotted in Figs. 14 and 15. The most important number is the dose seen in the first layer of the barrel pixel (BPix1) which is about 0.02±.01 Gy. Assuming 1 Gy of dose is equivalent to $3x10^9$ MIPs/cm^2 in Silicon, the dose in BPix1 corresponds to $6x10^7$ MIPs/cm^2. This is expected to come from 4-5 deflected bunches and in a span of about 100-125 ns. This dose/fluence is about the same as what we have calculated to be the dose/fluence in this layer in one second during normal pp operation at the nominal design luminosity of 10^{34} $cm^{-2}sec^{-1}$. The charged particle fluence in the layer will be about 10^8 cm^{-2}. The rate quickly falls off at higher radii as can be seen from Fig. 15. The dose and particle fluence at barrel pixel layer 2 is an order of magnitude lower. The dose averaged over the forward pixel layers 1 and 2 are about $2x10^{-4}$ Gy. Assuming the z-dependence in the volume of the pixel detector is flat and using the radial dependence of the dose in the barrel layers, the dose at the inner edge of FPIX layers is estimated to be $2x10^{-3}$Gy.

Table 1: Absorbed dose (Gy) and particle fluences (cm^{-2}) in various layers of the pixel and strip tracker detectors. (Errors are statistical only.) Acronyms used -- BPIX: Barrel Pixel, FPIX: Forward Pixel, TIB: Tracker Inner Barrel, TID: Tracker Inner Disk, TOB: Tracker Outer Barrel, TEC: Tracker EndCap

Sub. Det	Dose	Char. Had.	Neut. Had.	Muons	Electrons	Photons
BPIX1	(1.8±0.9) 10^{-2}	(1.1±0.6) 10^6	(2.3±1.2) 10^5	(5.1±2.6) 10^4	5.8 10^7	1.45 10^9
BPIX2	(1.1±0.3) 10^{-3}	(3.0±0.9) 10^5	(9.7±2.8) 10^4	(4.0±1.2) 10^4	3.3 10^6	1.10 10^7
BPIX3	(1.9±0.6) 10^{-4}	(1.4±0.4) 10^5	(3.6±1.2) 10^4	(3.5±0.2) 10^3	4.3 10^5	4.03 10^6
FPIX1	(2.3±0.4) 10^{-4}	(2.0±0.4) 10^5	(4.5±0.8) 10^4	(5.1±1.2) 10^4	4.6 10^5	1.41 10^7
FPIX2	(2.2±0.4) 10^{-4}	(1.6±0.2) 10^5	(1.8±0.4) 10^4	(3.8±0.2) 10^4	3.9 10^5	1.63 10^7
TIB1	(8.7±3.3) 10^{-5}	(4.1±1.6) 10^4	(2.2±0.8) 10^4	(7.1±2.7) 10^3	2.5 10^5	4.99 10^6
TIB2	(2.5±0.4) 10^{-5}	(2.3±0.3) 10^4	(1.1±0.2) 10^4	(1.9±0.3) 10^4	3.8 10^4	3.89 10^6
TIB3	(2.1±0.4) 10^{-5}	(1.4±0.2) 10^3	(7.9±1.3) 10^3	(1.9±0.3) 10^4	3.2 10^4	
TIB4	(1.6±0.2) 10^{-5}	(9.5±1.2) 10^3	(7.3±0.9) 10^3	(1.6±0.2) 10^4	1.8 10^4	
TID1	(7.7±4.8) 10^{-5}	(1.9±1.1) 10^4	(1.5±0.9) 10^4	(1.9±3.1) 10^4	2.5 10^5	3.41 10^6
TID3	(3.7±1.0) 10^{-5}	(1.6±0.4) 10^4	(1.3±0.3) 10^4	(1.8±2.1) 10^4	6.1 10^4	3.37 10^6
TOB1	(2.1±0.8) 10^{-5}	(7.6±3.0) 10^3	(8.2±3.0) 10^3	(1.6±0.6) 10^4	4.8 10^4	1.34 10^6
TOB2	(1.2±0.2) 10^{-5}	(3.7±0.5) 10^2	(6.0±0.5) 10^3	(1.5±0.2) 10^4	1.9 10^4	
TOB3	(1.1±0.2) 10^{-5}	(2.0±0.1) 10^3	(6.1±0.1) 10^3	(2.1±0.2) 10^4	1.6 10^4	
TOB4	(1.9±0.6) 10^{-5}	(1.9±0.6) 10^3	(5.6±0.1) 10^3	(1.9±0.6) 10^4	4.9 10^4	
TOB5	(1.0±0.1) 10^{-4}	(7.3±0.6) 10^2	(5.6±0.1) 10^3	(2.0±0.2) 10^4	3.9 10^5	
TOB6	(3.1±0.3) 10^{-5}	(5.2±0.4) 10^2	(5.5±0.1) 10^3	(1.8±0.1) 10^4	1.3 10^4	5.60 10^5
TEC1	(1.5±0.1) 10^{-5}	(4.7±0.4) 10^3	(7.2±0.5) 10^3	(1.8±0.2) 10^4	2.1 10^4	1.09 10^6
TEC9	(1.9±0.6) 10^{-5}	(2.1±0.7) 10^3	(9.6±3.1) 10^3	(1.9±0.6) 10^4	1.7 10^4	3.61 10^5

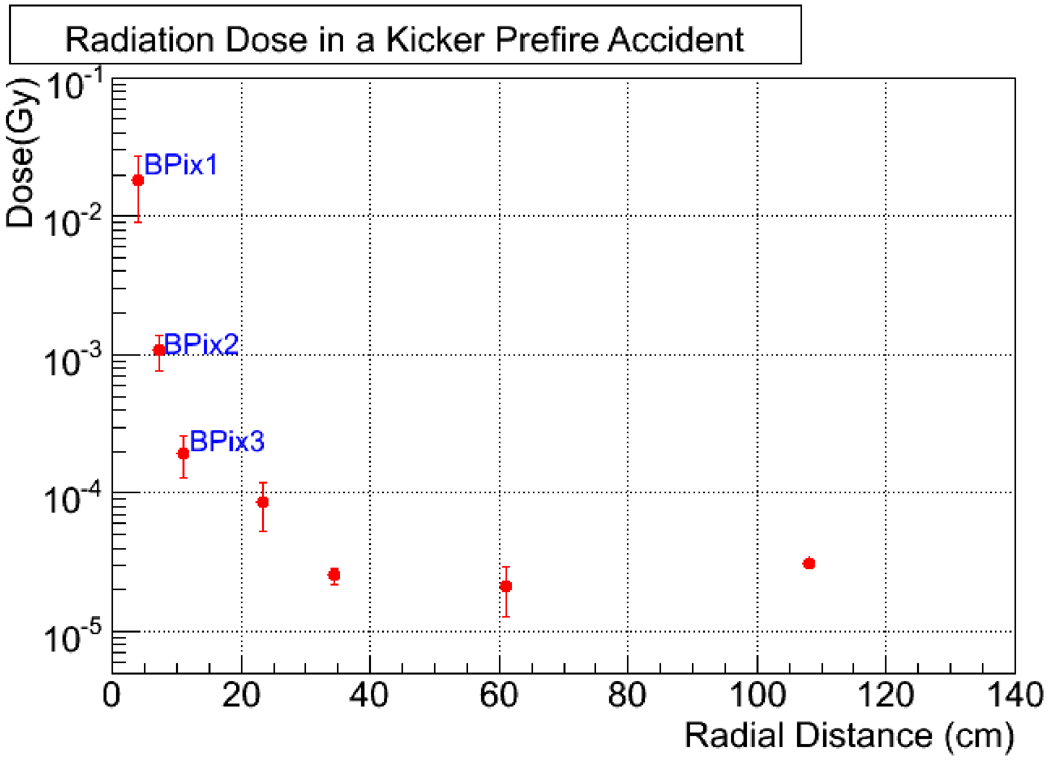

Fig. 14. Radial dependence of dose in the tracker.

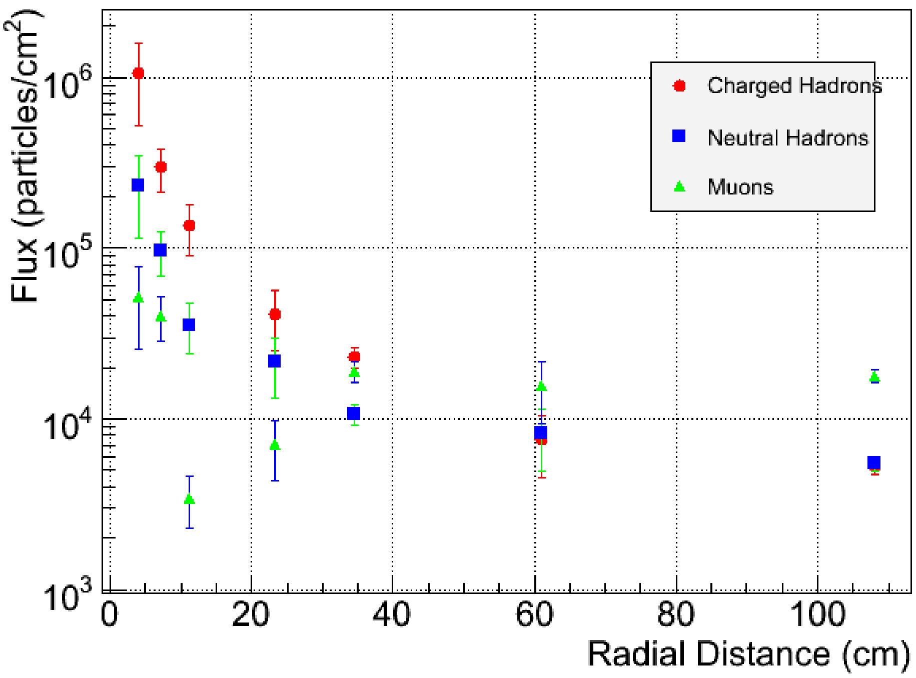

Fig. 15. Radial dependence of particle fluence in the tracker.

The energy spectra of charged and neutral hadrons are shown in Fig. 16 in some barrel and endcap (or forward) layers of the tracker. Spectra for electrons, positrons and photons are shown in Fig. 17. The layers closer to the beamline see high-energy particles. Energy spectra of muons are shown in Fig. 18. It is interesting to note that at very small radii, as the shower traverses through TAS absorber and other shielding close to the beamline, the fluence of muons falls. The muon fluence is higher and flatter at intermediate radii and tapers off at large radii as can be corroborated from Fig. 12.

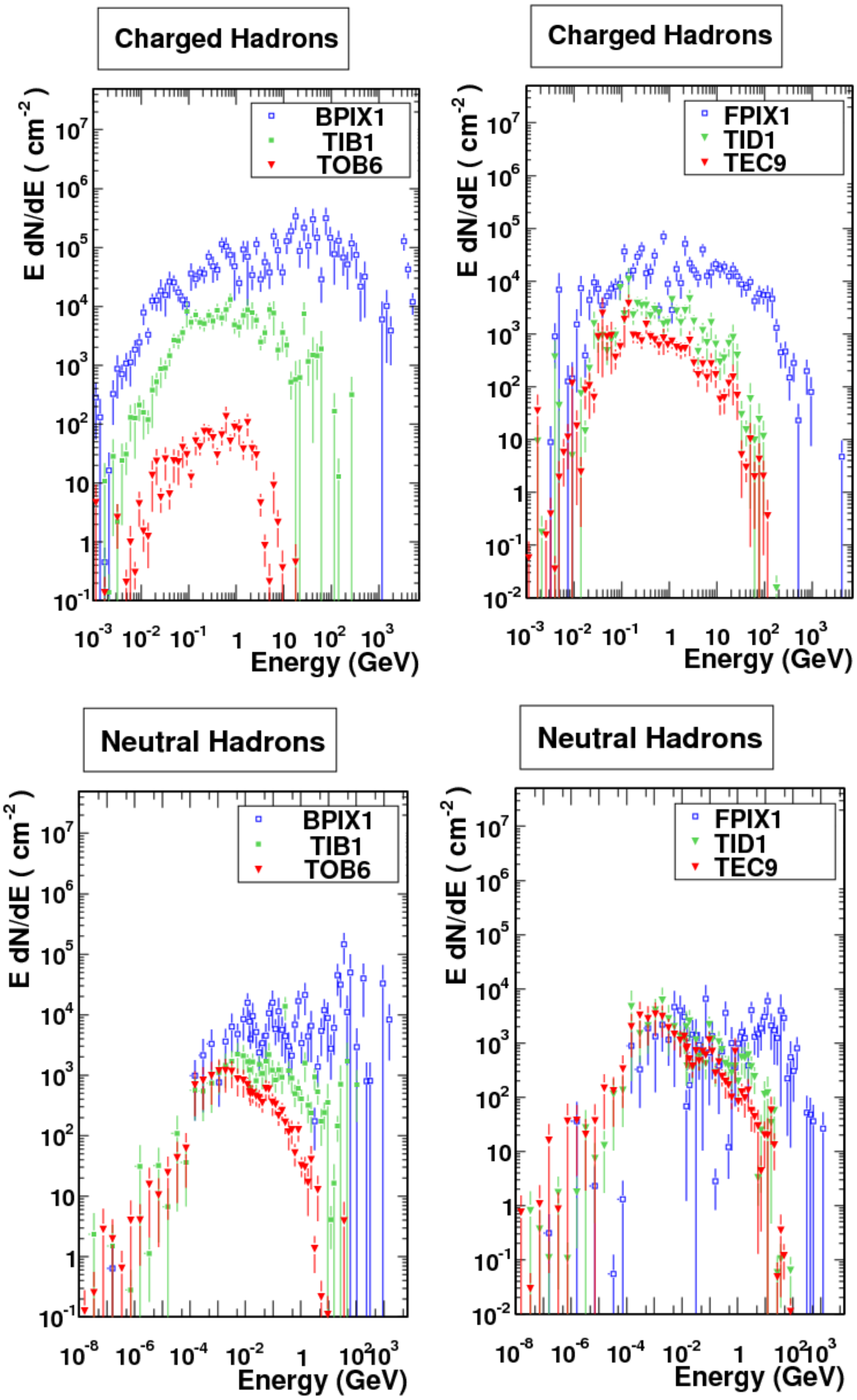

Fig. 16. Energy spectra of charged (top) and neutral (bottom) hadrons in the Pixel and SiTracker layers.

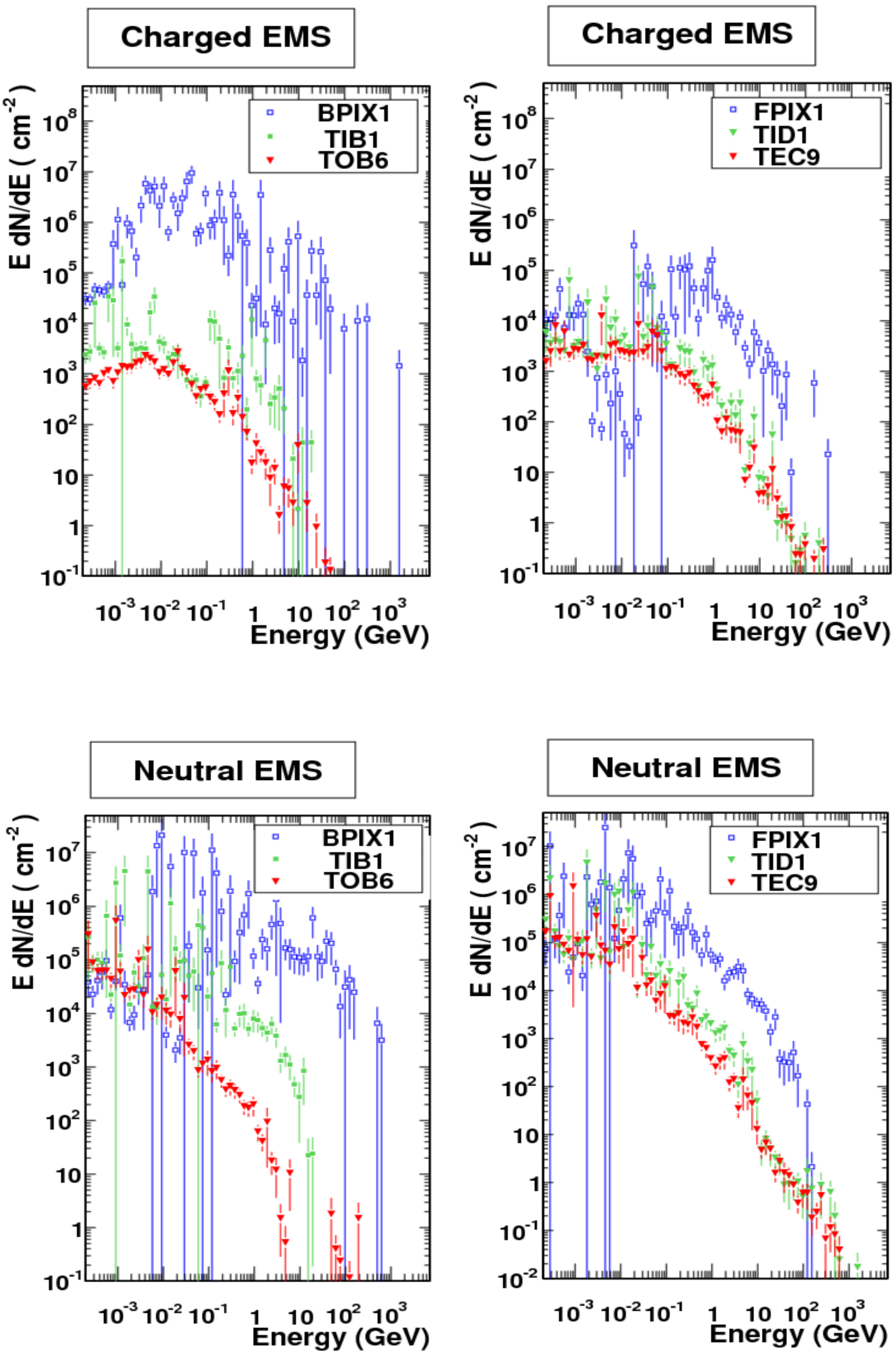

Fig. 17. Energy spectra of electrons and positrons (top) and photons (bottom) in the Pixel and SiTracker layers.

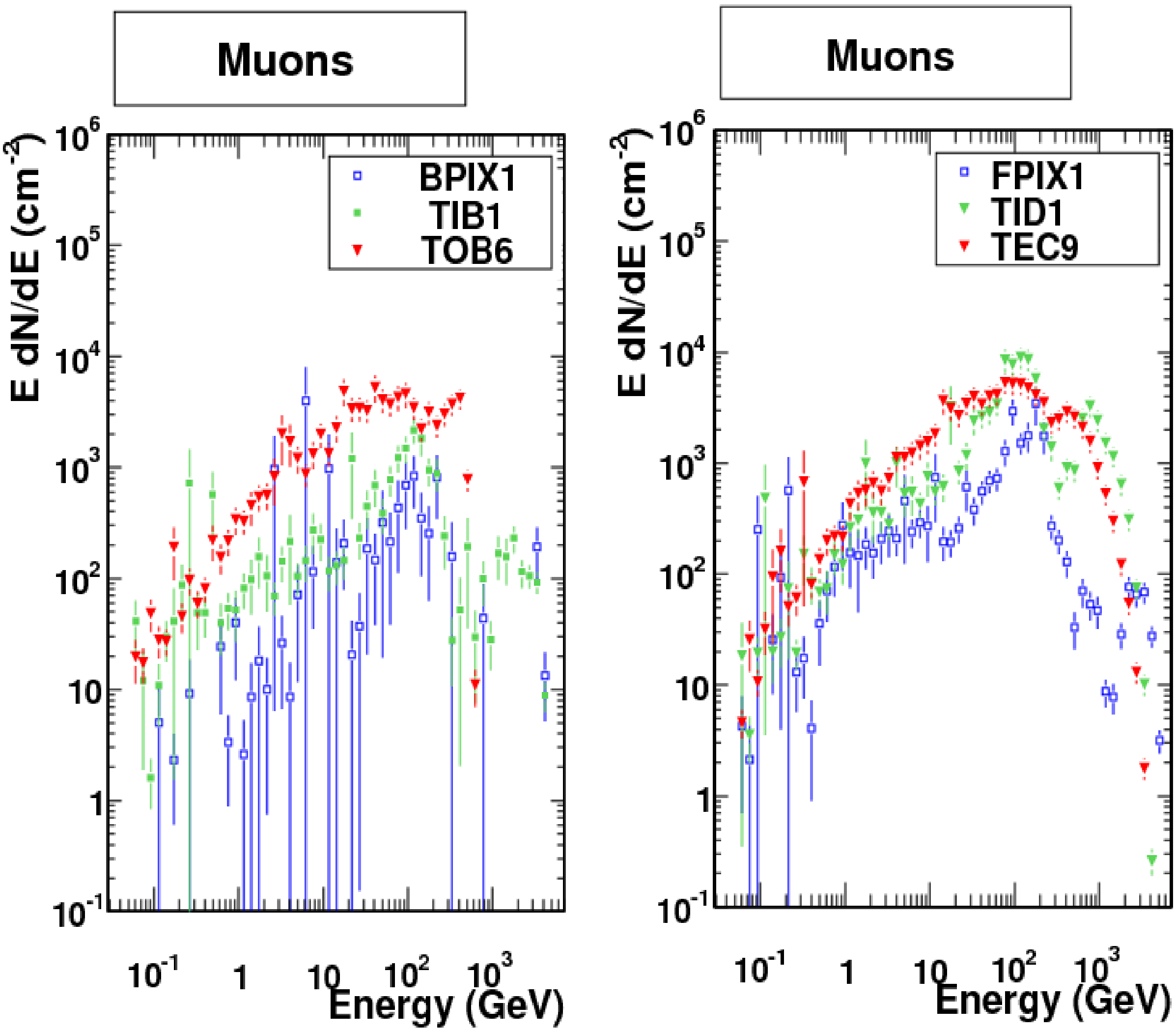

Fig. 18. Muon energy spectra in Pixel and SiTracker detectors.

6. Accidental Beam Loss on TAS

There are other beam accident scenarios that should be of concern to CMS where beam bunches are mis-injected or mis-steered. For example, incorrect injection settings of the dipole magnet D1 (see Fig. 3) can cause the incoming beam to scrape on the TAS absorber or the beam pipe close to the pixel detector. Such a scenario has been simulated and studied. The results are summarized in Tables 2 and 3. It is found that the dose in the first barrel pixel layer per proton scraping on TAS is about 5.6×10^{-10} Gy. This translates to a large dose of 56 Gy if a pilot bunch of 10^{11} protons are involved. However, it is very unlikely that 7 TeV protons could be mis-steered to hit the TAS. The collimators upstream of IP5 shadow TAS quite effectively. On the other hand, the 450-GeV beam, injected into the LHC from SPS, has some likelihood of being mis-steered onto TAS. In this case the dose seen at the barrel pixel is two orders of magnitude smaller, ~5×10^{-12} Gy/proton. This implies that if a single bunch of 10^{11} protons (say, a test pilot bunch) is lost on TAS, the dose can be 0.5 Gy (or 1.5E9 particles/cm^2), about 25 times larger than the dose from a single kicker prefire accident discussed so far. This is a likely accident and is more dangerous than a single-module kicker prefire and hence checks should be put in place to eliminate this risk.

Table 2: Absorbed dose (Gy) and particle fluences in layers of the pixel and strip tracker detectors for one 7-TeV proton lost on the TAS absorber at ~19 meters from IP5.

7 TeV p on TAS

	Dose (Gy/p)	Ch. Had. (/cm^2/p)	Neu. Had. (/cm^2/p)	Muons (/cm^2/p)
BPix1	**5.54E-10**	**7.40E-02**	**1.06E-02**	**1.28E-03**
BPix2,3+Fpix	**1.05E-10**	**1.98E-02**	**2.70E-03**	**1.06E-03**
TIB1	**1.47E-11**	**7.00E-03**	**7.50E-04**	**3.03E-04**
TOB1	**6.14E-12**	**1.92E-03**	**5.00E-04**	**1.57E-04**

Table 3: Absorbed dose (Gy) and particle fluences in layers of the pixel and strip tracker detectors for one 0.45-TeV proton lost on the TAS absorber at ~19 meters from IP5.

450 GeV p on TAS

	Dose (Gy/p)	Ch. Had. (/cm^2/p)	Neu. Had. (/cm^2/p)	Muons (/cm^2/p)
BPix1	**4.93E-12**	**1.84E-03**	**1.28E-03**	**9.60E-04**
BPix2,3+Fpix	**6.26E-12**	**2.36E-03**	**9.00E-05**	**5.40E-04**
TIB1	**2.32E-13**	**3.50E-04**	**9.20E-05**	**9.40E-06**
TOB1	**2.10E-13**	**1.25E-04**	**3.50E-05**	**7.34E-06**

7. Summary

We have presented results of detailed MARS15 simulations of the particle fluence and absorbed dose that can be seen in the CMS detector if a single module kicker pre-fire accident were to occur in the LHC. The impact on the pixel detector layers has been studied in particular since they are the most vulnerable in the event of such an accident. The dose seen in the first layer of the barrel pixel is about 0.02 Gy in ~120 ns, which is about the same as the dose in one second during pp-operation of the LHC at the design luminosity of 10^{34} $cm^{-2}sec^{-1}$. This is about 1000 times smaller than the previously estimated [3] dose before the tertiary collimators were introduced upstream of low-beta triplets in sector 5-6. The dose of 0.02 Gy is equivalent to a fluence of ~$6x10^7$ minimum ionizing particles/cm^2, in a time span of about 120 ns. No discernible damage to the pixel detectors or the electronics has been seen at these levels of fluence in recent beam tests. Therefore the conclusion from the study is that the single module kicker pre-fire, in the anticipated configuration with the tertiary collimators, is not expected to cause serious damage to the pixel detectors.

Our simulations of a mis-steered/mis-injected 450 GeV incoming beam hitting a TAS absorber ~19-m upstream CMS, shows this scenario to be more dangerous for the detector. A dose at BPIX1 of ~$5x10^{-12}$ Gy/proton can be seen or 0.5 Gy/pilot bunch of 10^{11} protons. This is a likely accident scenario if no action is taken. It can be avoided, however. Procedures must be put in place to ensure that the risk of this accident is eliminated.

8. Acknowledgements

The authors are thankful to Thomas Weiler for simulations that were used as input for the kicker prefire studies. We thank Jeff Spalding for many useful discussions.

One of the authors (Anil Singh) would like to thank the Fermilab LPC for support during his stay at Fermilab and Prof. S. Beri (Panjab University) for encouragement and support.

References

[1] The CMS experiment at the CERN LHC, The CMS Collaboration, S Chatrchyan *et al,* 2008, JINST 3 S08004.
[2] N.V. Mokhov, T. Weiler, "Machine-Induced Backgrounds: Their Origin and Loads on ATLAS and CMS", Fermilab-Conf-08-147-APC, May 2008, to be published in Proc. of the Workshop on Experimental Conditions and Beam Induced Detector Backgrounds, April 3-4, 2008, CERN, Switzerland.
[3] A.I. Drozhdin, N.V. Mokhov, M. Huhtinen, "Impact of the LHC Beam Abort Kicker Prefire on High-Luminosity Insertion and CMS Detector Performance", Fermilab-Conf-99/060 (1999), Proc. of the 1999 Particle Accelerator Conference, N.Y., 1999, p. 1231.
[4] N.V. Mokhov, "The Mars Code System User's Guide", Fermilab-FN-628 (1995); N.V. Mokhov, S.I. Striganov, "MARS15 Overview", in *Proc. of Hadronic Shower Simulation Workshop*, Fermilab, September 2006, AIP Conf. Proc. 896, p. 50 (2007); Fermilab-Conf-07/008-AD (2007); http://www-ap.fnal.gov/MARS/.
[5] G. Robert-Demolaize, et al., "A New Version of SIXTRACK with Collimation and Aperture Interface", PAC'05, Knoxville, Tennessee, 2005.
[6] N.V. Mokhov, A.I. Drozhdin, I.L. Rakhno, M. Gyr, E. Weisse, "Protecting LHC Components against Radiation Resulting from an Unsynchronized Beam Abort", Proc. PAC'01, p. 3168, Chicago, 2001; Fermilab-Conf-01/133 (2001).
[7] R. Assmann et al., "The Consequences of Abnormal Beam Dump Action on the LHC Collimation System", LHC-Project-Note-293, 2002.